The differential equation (2.1) becomes

$$d^2i/dt^2+(i/LC_0)[1-\sum_{n=1}^{\infty}(C_n/C_0)\cos 2n\omega t]=0. \quad (2.4)$$

This equation is the Hill equation and would be quite cumbersome to solve. Fortunately, it is possible to augment mathematics with physical intuition to simplify the problem considerably. It is convenient to introduce the concept of "tuning" the inductor, L, in the resonant circuit. This consists of deemphasis of all but one of the terms in the series; i.e., Eq. (2.4) can be approximated by

$$d^2i/dt^2+(i/L_nC_0)[1-(C_n/C_0)\cos 2n\omega t]=0. \quad (2.5)$$

In other words, by choosing L_n to resonate with C_0 at the harmonic of the driving frequency a process of selective filtering results. Equation (2.5) is, of course, the Mathieu equation and its solution is to a good approximation:

$$i=I_n\cos n\omega t \quad n=1, 2, 3\cdots. \quad (2.6)$$

Thus a means of frequency multiplication by odd and even integers is obtained.

CONCLUSIONS

A novel ferroelectric device has been described, and a theory of operation derived. The even symmetry of the *C versus V* curve of Fig. 3 causes the periodic variation of $C(t)$ to contain only even harmonics of the driving frequency. Subsequently, a frequency division by two occurred through the mechanism of the Mathieu equation.

The coupling between the two pairs of orthogonal plates here originated in the nonlinear property of the dielectric used. The dielectric is assumed to be homogeneous and isotropic. If a piezoelectric material is used, is is readily seen that electromechanical modulation can occur. That is, application of voltage across one pair of plates can actually change the capacitance across the other pair by virtue of a mechanical deformation.

Further applications of the device described is currently limited by the "mild" nonlinearities of available ferroelectrics. The interaction theory here described can readily be extended to the general case of a modulator with three pairs of mutually orthogonal plates.

JOURNAL OF APPLIED PHYSICS VOLUME 27, NUMBER 7 JULY, 1956

Theoretical Considerations Governing the Choice of the Optimum Semiconductor for Photovoltaic Solar Energy Conversion*†

JOSEPH J. LOFERSKI
Radio Corporation of America, RCA Laboratories, Princeton, New Jersey

(Received January 7, 1956)

The theory of the photovoltaic effect is used to predict the characteristics of a semiconductor which would operate with an optimum efficiency as a photovoltaic solar energy converter. The existence of such an optimum material results from the interaction between the optical properties of the semiconductor which determine what fraction of the solar spectrum is utilized and its electrical properties which determine the maximum efficiency of conversion into electricity. Considerable attention is devoted to the effect of the forbidden energy gap (E_G) of the semiconductor. It is shown that atmospheric absorption causes a shift in the solar spectrum which changes the value of the optimum forbidden energy gap between the limits 1.2 ev$<E_G<$1.6 ev. Furthermore, plausible departures of the diode reverse saturation current (I_0) from the parametric dependence predicted by Shockley are considered, and it is shown that such departures reduce the advantage of the optimum material over others in the range 1.1 ev$<E_G<$2.0 ev. The relation between E_G and the load impedance for maximum power transfer from the solar converter is discussed. Finally, I_0 is computed from the published values of the semiconductor parameters of three intermetallic compounds, i.e., InP, GaAs, and CdTe, and it is shown that the efficiencies predicted for these materials are greater than those predicted for other materials which have been proposed, i.e., Si, CdS, Se, and AlSb.

INTRODUCTION

THE purpose of this investigation was to find that semiconductor which, when it is used in a photovoltaic cell, will convert solar energy into electricity with the highest theoretical efficiency. An investigation such as this had become desirable because there appeared to be some confusion in the literature concerning the best semiconductor for such application. Thus, both Si[1] and CdS[2] have been recently proposed as practical solar energy converters. Furthermore, Cummerow[3] states that the optimum material should have $E_G=2$ ev. On the other hand, Rittner[4] recommends a material

* The work described in this report was performed under contract with the U. S. Signal Corps Engineering Laboratory, Fort Monmouth, New Jersey.

† The contents of this article are essentially the same as that of a paper presented at the Conference on Solar Energy, Tucson, Arizona, November 1, 1955.

[1] Chapin, Fuller, and Pearson, J. Appl. Phys. **25**, 676 (1954).
[2] D. C. Reynolds, and G. M. Leies, Elec. Eng. **73**, 734 (1954).
[3] Robert L. Cummerow, Phys. Rev. **95**, 16 (1954).
[4] E. S. Rittner, Phys. Rev. **96**, 1708 (1954).

whose E_G is between 1.5 and 1.6 ev. Furthermore, Rittner shows that optimum material is shifted slightly between these limits by increasing the concentrations of donors and acceptors. He concludes that AlSb should be superior to silicon. Finally Prince[5] shows the optimum occurring at about 1.3 ev with only a very small difference between the efficiency for Si and for this optimum material.

Our analysis considers certain refinements not included in the other three. First of all, instead of approximating the solar spectrum by that of a blackbody, we have used published data on the distribution of solar energy and how it is affected by absorption in the atmosphere. Secondly, we have considered a number of plausible departures from the simple theory of rectification for p-n junctions. Finally, we have computed efficiencies for some materials whose technology is sufficiently advanced to permit experiments to be made on them.

ANALYSIS OF THE PHOTOVOLTAIC EFFECT

The theory of p-n junction photovoltaic cells has been presented elsewhere.[6–9] It has been shown that the irradiated p-n junction is equivalent to a constant current generator producing a current I_s in parallel with a nonlinear impedance, whose i-V characteristic is given by

$$I_j = I_0(\epsilon^{\lambda V} - 1), \tag{1}$$

where I_0 is the reverse saturation current and $\lambda = e/kT$. (It has been found in practice, however, that $\lambda = e/AkT$ where $A > 1$,[9] although there is some evidence that λ may be given by $\lambda^{-1} = kT/e + b$ where b is a constant[10].) If a matching load is connected across the junction, the voltage at maximum power transfer, V_{mp}, is given by

$$\epsilon^{\lambda V_{mp}}(1+\lambda V_{mp}) = \frac{I_s}{I_0} + 1 = \epsilon^{\lambda V_{\max}}, \tag{2}$$

where $V_{\max}$ is the open circuit voltage. To compute V_{mp} it is therefore necessary to determine I_0 and I_s. The former can be computed from the theory of p-n junctions as indicated below. The I_s, on the other hand, can be computed from the relation

$$I_s = Q(1-r)(1-\epsilon^{-\alpha l})en_{ph}(E_G), \tag{3}$$

where Q is the collection efficiency defined as the ratio of the carriers passing through the circuit to those which have been generated in the bulk, r is the reflection coefficient, $\epsilon^{-\alpha l}$ is the fraction of the radiation transmitted, α is the absorption constant, l is the thickness of the absorbing semiconductor, e is the electronic charge, and $n_{ph}(E_G)$ is the number of photons per second per unit area of p-n junction whose energy is great enough to generate hole-electron pairs in the semiconductor.

Finally, it can be shown that the maximum efficiency, $\eta_{\max}$, which is defined as the ratio of the maximum electrical power output to the solar power arriving on unit area, is given by

$$\eta_{\max} = Q(1-r)(1-\epsilon^{-\alpha l})\frac{\lambda V_{mp}}{(1+\lambda V_{mp})}\frac{en_{ph}(E_G)}{N_{ph}}\frac{V_{mp}}{E_{Av}}, \tag{4}$$

where N_{ph} is the total number of photons in the solar spectrum and E_{Av} is the average energy of such photons. Since $n_{ph}(E_G)$ decreases with E_G, while the ratio I_s/I_0 and, consequently, V_{mp} (Eq. (2)) increase with E_G, it is evident that $\eta_{\max}$ will pass through an optimum as a function of E_G.

In the analysis outlined above it is assumed that the internal shunt resistance is much greater than R_L and that the internal series resistance is much less than R_L, where R_L is the load resistance across the junction. The first condition is easy to achieve, but the second can seriously reduce $\eta_{\max}$. It will be shown that in materials with E_G greater than that of Si, the series resistance may be less troublesome.

COMPUTATION OF I_s

(i) $n_{ph}(E_G)$

The spectral distribution of the radiation reaching the earth from the sun can be approximated by that of a

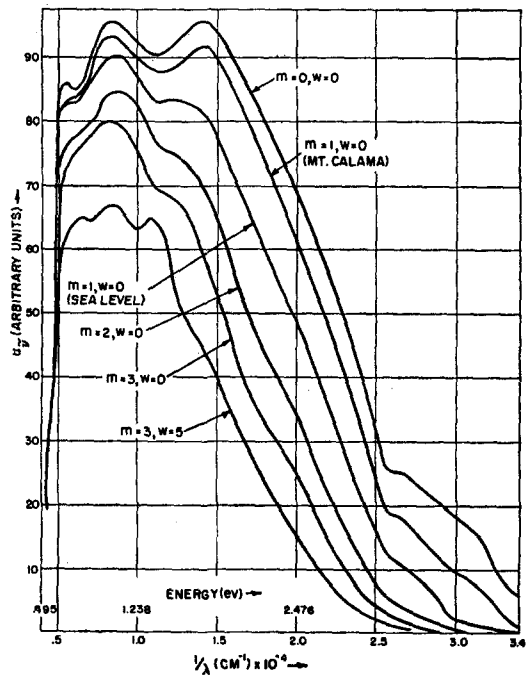

FIG. 1. Solar spectrum for different absorption conditions.

[5] M. B. Prince, J. Appl. Phys. **26**, 534 (1955).
[6] J. N. Shive, Proc. Inst. Radio Engrs. **40**, 1410 (1952).
[7] Paul Rappaport, Phys. Rev. **93**, 246 (1954).
[8] Rappaport, Loferski, and Linder, R C A Rev **17**, 100 (1956).
[9] W. Pfann and W. van Roosbroeck, J. Appl. Phys. **25**, 1422 (1954).
[10] H. Kleinknecht and K. Seiler, Z. Physik **Bd139**, 599 (1954).

blackbody at a temperature of 5900°K. However, there is a sufficient departure from this idealized spectrum to make it desirable to use more exact data. Such data have been compiled principally by C. G. Abbott and others at the Smithsonian Institution.[11–13] Their results are published in the form of the spectral distribution outside the atmosphere and the absorption constants associated with the three sources of atmospheric absorption—namely, (a) atmospheric gases (O_2, N_2, etc.), (b) aqueous vapor, and (c) dust. All of these absorption mechanisms tend to deplete the ultraviolet wavelengths preferentially. Their effect can be described by means of the optical path length, m, through which the light passes and by means of the number of cm, w, of precipitable water vapor in the atmosphere. The parameter m is defined by the relation $m=1/\cos\theta$ where θ is the angle between the line drawn through the observer and the zenith and the line through the observer and the sun. During the course of a day θ varies from 90° to a minimum, $\theta_{\min}$, which occurs at noon. Furthermore, $\theta_{\min}$ varies with the season of the year between the limits $\theta_{\min}=\text{latitude}\pm 23.50°$. There is therefore an appreciable variation in m, and the resulting shift in spectral distribution is shown in Fig. 1. Here we have plotted $u_{\tilde{\nu}}$, the intensity per unit wave number per cm² *vs* $\tilde{\nu}=1/\lambda$. We have also included for convenience an energy scale in electron volts. The curve outside the atmosphere can be normalized by setting the total area included under it equal to the solar constant. Abbott's value of 1.94 cal/min/cm² (0.135 w/cm²) has been used throughout the calculation. All the other curves shown in Fig. 1 can be normalized relative to the curve for the outer atmosphere.

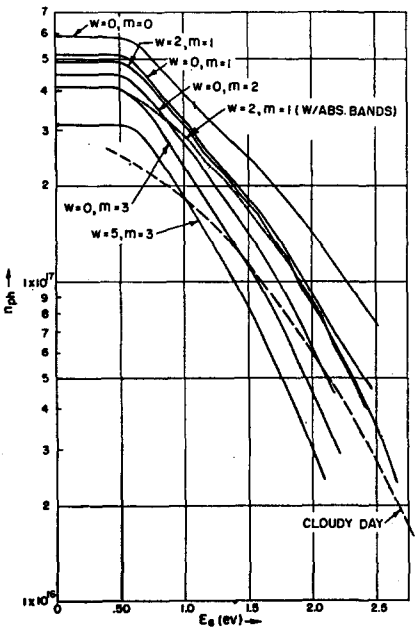

FIG. 2. Potential number of absorbed photons *vs* energy of cut-off (absorption edge).

TABLE I. Parameters of the solar spectrum as a function of absorption conditions.

m	w	Comments	U (w/cm²)	E_{Av} (ev)	N_{ph} (No./sec/cm²)
0	0	Outside atmosphere	0.135	1.48	5.8×10^{17}
1	0	Sea level, sun at zenith	0.106	1.32	5.0×10^{17}
2	0	Sea level, sun at 60° from zenith	0.088	1.28	4.3×10^{17}
3	0	Sea level, sun 70.5° from zenith	0.075	1.21	3.9×10^{17}
1	2	Without selective absorption bands	0.103	1.25	4.8×10^{17}
1	2	With selective absorption bands	0.089	1.43	3.9×10^{17}
3	5	Most extreme conditions	0.059	1.18	3.2×10^{17}
1	0	Cloudy day (7000° blackbody)	0.012	1.44	5.2×10^{16}

The effect of absorption by aqueous vapor is shown by one of the curves in Fig. 1 for the case $w=5$, $m=3$, which can be considered as the extreme shift in the spectrum which can be produced by absorption in the atmosphere. Calculations have also been made for the case $w=2$, which corresponds to a relative humidity of about 50%[14] in which we have also included absorption due to the selective absorption bands in the atmosphere.

Since the literature does not contain any tabulated data for the spectrum on a cloudy day comparable to that discussed in the foregoing, this condition was approximated, following Kimball, by using the spectral distribution for a blackbody at 7000°K and modifying it by atmospheric absorption corresponding to $m=1$ and $w=0$.

It is now possible to compute $n_{ph}(E_G)$ by counting those photons whose energy exceeds the energy gap of the material, E_G, i.e.,

$$n_{ph}(E_G)=\sum_{\nu=E_G/h}^{\nu=\nu_{\max}} n_{ph}(\nu), \tag{5}$$

where $n_{ph}(\nu)$ was chosen to be the number of photons of energy $h\nu$ in the intervals $\Delta(1/\lambda)=10^{-5}$ cm^{-1} and $\nu_{\max}$ is the maximum frequency in the solar spectrum. The result is shown in Fig. 2, where $n_{ph}(E_G)$ is plotted *vs* E_G. The total number of solar photons, N_{ph}, is computed by summing from $\nu=0$ to $\nu=\nu_{\max}$. Finally E_{Av} is determined from the relation, $U=N_{ph}E_{Av}$, where U is the total energy content of the solar spectrum.

In Table I, we have recorded as a function of m and w the power received (for normal incidence) in w/cm², the average energy of a photon, E_{Av} and the total number of photons in the spectrum N_{ph}, all of these quantities being computed as indicated above.

[11] Abbott, Fowle, and Aldrich, Smithsonian Misc. Collections N9, 74, 7 (1923).
[12] H. H. Kimball, Proc. Internatl. Conf. Illumination, 501 (1928).
[13] W. Forsythe, "Measurement of radiant energy." The solar spectrum and $a_{a\lambda}a_{d\lambda}$ are tabulated by C. G. Abbott on page 77.

[14] We are indebted to Dr. Aufen Kampe, meterologist at the Signal Corps Laboratory, for discussions of the computation of w.

(ii) Reflection Losses

To estimate the magnitude of reflection losses one can use the relation between the index of refraction, n and r, namely,

$$r=(n-1)^2/(n+1)^2. \quad (6)$$

By using the index of refraction for wavelengths beyond the absorption edge it is possible to get a reasonable estimate of r. However, n has not been measured for many of the materials of possible interest. It must therefore be estimated from the empirical relation due to Moss,[15] namely,

$$E_G n^4=173, \quad (7)$$

which is approximately true for materials of the zinc blende or diamond lattice structure. From this expression we find that if $E_G=1.0$ ev, $n=3.6$, and $r=0.31$ and if $E_G=1.5$ ev, $n=3.3$ and $r=0.29$. Thus, we do not expect any significant difference in reflection losses for materials in the range of values for E_G in which we are principally interested. Consequently, it does not appear that reflection losses will influence the choice of the best material for solar converters.

(iii) Collection Efficiency, Q

All the minority carriers which are generated in the solid by the radiation do not contribute to the power developed in the load, because some of them recombine with majority carriers either inside the volume or at the surface. This phenomenon has been introduced into the theory by defining a collection efficiency, Q, which is the ratio of the carriers passing through the circuit (i.e., the experimentally measured short circuit current, I_s) to the total number of carriers generated in the solid per unit time, thus

$$Q=\frac{I_s}{(1-r)(1-\epsilon^{-\alpha l})e n_{ph}(E_G)}. \quad (8)$$

Q can be computed for a simple geometry such as that shown in Fig. 3,[8] which shows an infinite plane p-n junction at $x=l$ with the n region extending from $x=0$ to $x=l$. Q is a function of the absorption constant for the radiation, α, the minority carrier lifetime, τ, and the surface recombination velocity, s. Q has been computed for some representative values of these parameters to illustrate the range of values it can assume for the materials under discussion. The results are tabulated in Table II. It should be pointed out that the values of Q would be somewhat higher if generation in both sides of the junction had been included in the calculation.

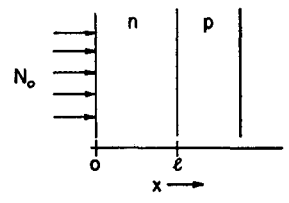

FIG. 3. Geometry for the computation of Q.

TABLE II. Collection efficiency, Q, for different combinations of s, L, and α.

s(cm/sec)	L(cm)	α(cm^{-1})	l(cm)	Q
0	10^{-2}	10^3	10^{-3}	0.61
0	10^{-3}	10^3	10^{-3}	0.47
0	10^{-3}	10^6	10^{-3}	0.65
0	10^{-6}	10^3	10^{-3}	6×10^{-5}
100	10^{-3}	10^3	10^{-3}	0.61
∞	10^{-2}	10^3	10^{-3}	0.25
∞	10^{-3}	10^3	10^{-3}	0.23
∞	10^{-3}	10^6	10^{-3}	0.001
∞	10^{-6}	10^3	10^{-3}	6×10^{-5}

It is evident from this table that the most favorable condition for collecting the generated carriers is that for which $l/L\ll1$ and for which the surface recombination velocity, s, has a low value. To estimate the magnitude of s and L required to maintain high Q, note that the absorption constant, α, will lie in the range 10^4 cm^{-1} $<\alpha<10^6$ cm^{-1} for radiation near the absorption edge. For efficient absorption it is necessary that $l\approx\alpha^{-1}$, i.e., 10^{-4} cm $<l<10^{-6}$ cm. If $l=0.1$ L and since $L=(D\tau)^{\frac{1}{2}}$, where L is the diffusion length, D is the diffusion constant assumed to be 10 cm^2/sec and τ is the lifetime of minority carriers, τ should lie in the range 10^{-7} sec $>\tau>10^{-11}$ sec. As for the requirements on s, it can be shown[8] that s will not reduce Q if $s/D\ll1/L$ and $s/D\ll\alpha$. With $l=0.1L=\alpha^{-1}$ both these conditions are satisfied if $s<10^5$ cm/sec for α in the range indicated above. It appears reasonable to assume therefore that with such moderate requirements on τ and s there are many materials which should be capable of high values of Q when they are used in photovoltaic cells. Consequently, the attainable value of Q should not affect the choice of the best material for solar conversion.

COMPUTATION OF I_0

As the basis for the computation, we have used Shockley's expression for I_0,[16] which can be written as

$$I_0=A\epsilon^{-E_G/kT} \quad (9)$$

with

$$A=\frac{b}{(1+b)^2}kT(\mu_n+\mu_p)\left(\frac{1}{\sigma_n L_p}+\frac{1}{\sigma_p L_n}\right)(N_c N_V)^{\frac{1}{2}}. \quad (10)$$

The A was computed for silicon, using the values for the parameters compiled by Conwell,[17] with the assumptions that $\sigma_n L_p\ll\sigma_p L_n$ and that $\sigma_n L_p=5.3\times10^{-2}\Omega^{-1}$. Using these values we find that

$$I_{01}=1.44\times10^8\epsilon^{-E_G/kT}. \quad (11)$$

[15] T. S. Moss, *Photoconductivity in the Elements* (Academic Press, Inc., New York, 1952), p. 244.

[16] William Shockley, Bell System Tech. J. **28**, 435 (1949).

[17] E. M. Conwell, Proc. Inst. Radio Engrs. **40**, 1327 (1952).

It is from this expression that I_0 is computed as a function of E_G for most of the calculations to follow. (Those values of I_0 which have been computed from Eq. (11) will be identified by the subscript 1.)

Using Eqs. (9) and (10), I_0 has been computed from the known values of μ_n, μ_p, L_p, L_n, etc., for a limited number of materials, namely, Si, InP, GaAs, and CdTe. In Table III, we have tabulated these values of I_0 and the corresponding values of $\eta_{\max}$. The values of E_G, μ_n, and μ_p are taken from those given by Welker[18] and Jenny,[19] except those for Si which are taken from Conwell. The value of τ_p is an estimated upper limit on this quantity.

Two plausible departures of I_0 from the dependence shown in Eq. (9) have been considered.

(1) It was assumed that the actual I_0 was given by the expression

$$I_{02}=1.44\times10^{8}f\epsilon^{-E_G/kT}. \tag{12}$$

(Reverse currents computed from this formula will be identified by the subscript 2.) We considered the case $f=10^n(-5<n<5)$. Such a change in I_0 can occur if the product $\sigma_n L_p$ departs from the assumed value $5.3\times10^{-2}\Omega^{-1}$ by a factor $1/f$. Such changes in I_0 will also occur for a material whose values of μ_n, μ_p, m_n, and m_p differ from those of Si, but order-of-magnitude changes are more likely to result from changes in the $\sigma_n L_p$ product.

(2) It was assumed that

$$I_{03}=\epsilon^{-E_G/kT}. \tag{13}$$

(Reverse currents computed from this formula will be referred to by the subscript 3.) A dependence on E_G such as that shown in I_{03} has been reported for grown Si junctions by Kleinknecht[10] and for the n-i-p Ge junction by Hall.[20] The literature does not show any evidence for an $I_0\propto\exp-E_G/kT$ in Si or for that matter in any material except Ge. It is for this reason that we have included I_{03} in the analysis.

COMPUTATION OF $\eta_{\max}$

To compute $\eta_{\max}$ it is only necessary to form the ratio I_s/I_0 for the different spectra and to determine λV_{mp} from Eq. (2). To simplify the calculation, we have neglected reflection, transmission, and recombination losses, which are not expected to vary appreciably among the different materials. As indicated above the effect of these losses will be to reduce the attainable $\eta_{\max}$ by a factor which will probably not exceed 0.9. Throughout the computation, we have used $\lambda=e/kT$ in spite of the known departures of λ from this expression. The results of the computation are shown in Figs. 4 through 10. The figures include vertical lines at the values of E_G for Si and for InP, GaAs, and CdTe which appear to be the most promising materials on which experimental work is possible at this time.

TABLE III. I_0 and $\eta_{\max}$ for Si, InP, GaAs, and CdTe.

Material	E_G (ev)	μ_n (cm²/ v sec)	μ_p (cm²/ v sec)	τ_p (sec)	N_D (cm⁻³)	I_0 (amp/cm²)	$\eta_{\max}$ $m=0$ $w=0$	$\eta_{\max}$ $m=1$ $w=2$
Si	1.12	1200	250	10^{-5}	10^{17}/cc	5.9×10^{-12}	19.4%	20.3%
InP	1.25	3000	600	10^{-8}	10^{17}/cc	1.9×10^{-14}	21.1%	22.4%
GaAs	1.35	3000	600	10^{-8}	10^{17}/cc	4.1×10^{-16}	22.4%	23.7%
CdTe	1.45	300	30	10^{-8}	10^{17}/cc	1.2×10^{-19}	26.6%	26.5%

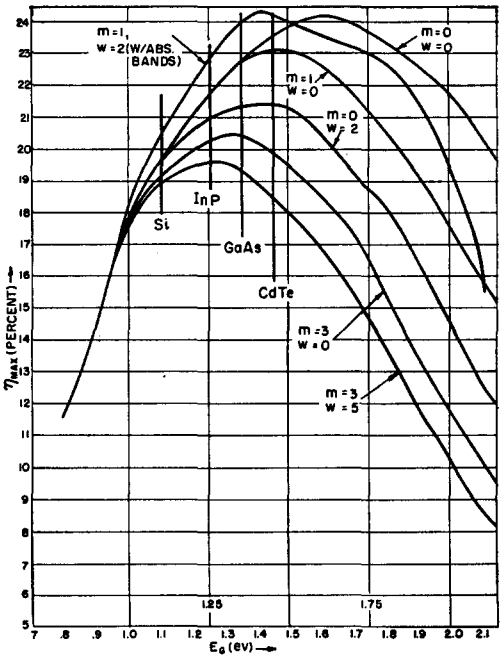

FIG. 4. $\eta_{\max}$ *vs* E_G for different absorption conditions with $I_0=I_{01}$.

Figure 4 shows $\eta_{\max}$ *vs* E_G for different conditions of atmospheric absorption. These curves show that the optimum value of $\eta_{\max}$ occurs for progressively lower values of E_G as absorption by the atmosphere increases. Furthermore, the difference between the optimum $\eta_{\max}$ and the value of $\eta_{\max}$ for Si decreases with increasing absorption.

Figure 5 shows $\eta_{\max}$ *vs* E_G for different values of m and w where the effect of including selective absorption bands due to aqueous vapor is included. Because these bands occur on the low-energy side of the spectrum, it is evident from this figure that they produce very little change in the $\eta_{\max}$ *vs* E_G curve although they do reduce the total power received.

Figure 6 shows $\eta_{\max}$ *vs* E_G for a cloudy day which was approximated as discussed above. Two values for the power input, i.e., 0.060 w/cm² and 0.012 w/cm² are included in the curve to show that $\eta_{\max}$ does not decrease very much with power input at levels of mw/cm².

Figure 7 shows a comparison between $\eta_{\max}$ *vs* E_G curves for $I_{01}\propto\exp(-E_G/kT)$ and those for $I_{03}\propto\exp(-E_G/2kT)$. $I_s(E_G)$ was computed for $m=1$, $w=2$. Although the optimum $\eta_{\max}$ occurs at roughly the

[18] H. Welker, Scientia Elect. **1**, 2 (1954).
[19] D. A. Jenny and R. H. Bube, Phys. Rev. **96**, 1190 (1954).
[20] R. N. Hall, Proc. Inst. Radio Engrs. **40**, 1512 (1952).

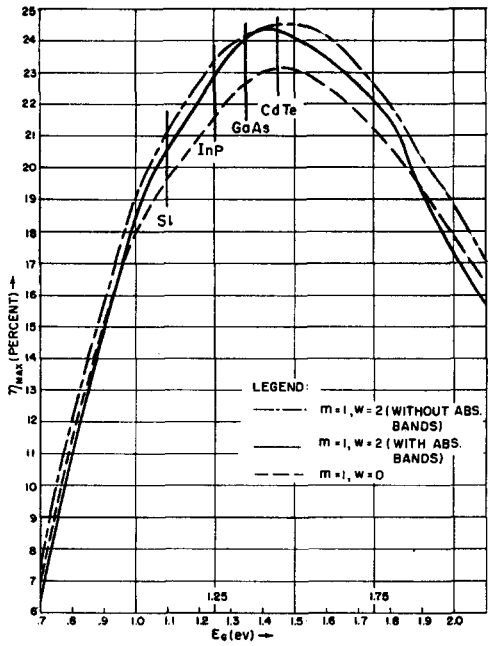

FIG. 5. $\eta_{\max}$ *vs* E_G showing the effect of absorption by H_2O vapor.

same value of E_G on both curves, the difference between the optimum $\eta_{\max}$ and that for silicon has become almost negligible, in the case of I_{03}.

Figure 8 shows

$$\eta_{\max} \text{ vs } \ln(I_{02}/I_{01}) = \ln f = n \ln 10 (-5 < n < 5)$$

for different values of E_G. The resulting straight lines have slopes which decrease with increasing E_G. The result of this behavior is that the optimum $\eta_{\max}$ occurs for different values of E_G as f increases. The slopes of the lines in Fig. 8 are proportional to I_s which can be shown by examining the expression for $\eta_{\max}$, Eq. (4). It can be shown that $i_{mp} \sim I_s$ and $V_{mp} \sim V_{\max}$, so that we can approximate $\eta_{\max}$ by

$$\eta_{\max} \sim \frac{I_s \ln(I_s/I_{02})}{N_{ph} E_{Av} \lambda} = C I_s \ln(I_s/I_{01} f). \qquad (14)$$

Consequently, the slope of the lines in Fig. 8 is CI_s. Since $I_s = e\, n_{ph}(E_G)$ decreases with increasing E_G, the slopes have the behavior discussed in the foregoing.

In order to illustrate this point further, the shift in the optimum $\eta_{\max}$ is shown in Fig. 9. It is evident in these plots, that the $\eta_{\max}$ *vs* E_G curve shifts as a unit toward larger values of E_G with increasing f. Furthermore, $\eta_{\max}$ decreases in magnitude, since I_s/I_0 has been

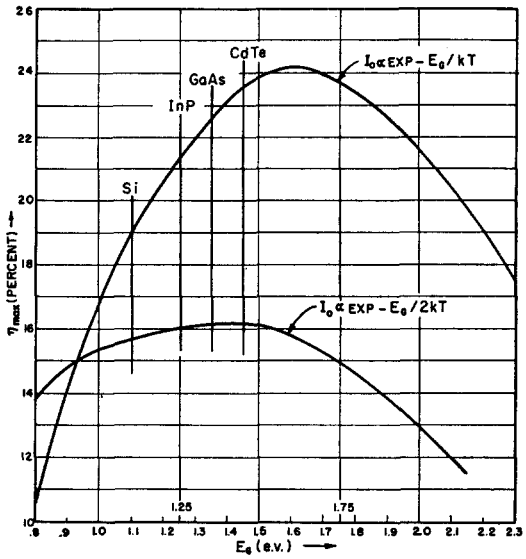

FIG. 7. $\eta_{\max}$ *vs* E_G outside atmosphere ($m=0$, $w=0$) showing the effect of relation between I_0 and E_G.

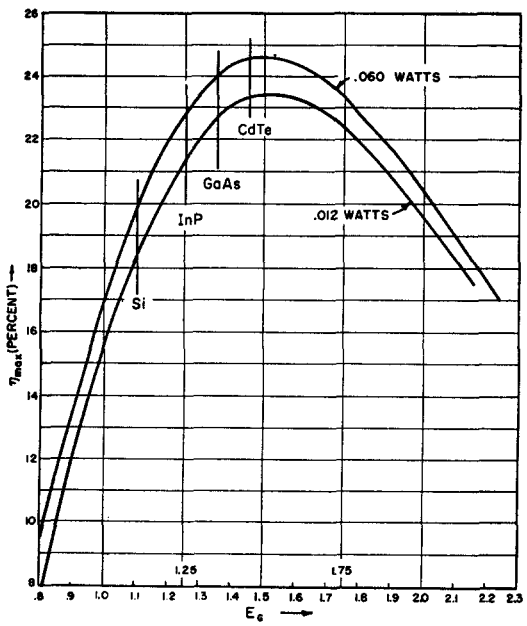

FIG. 6. $\eta_{\max}$ *vs* E_G for cloudy day ($m=1$, $w=0$) with two different values of U.

lowered by the factor $1/f$. Such changes in f can arise from changes in any of the parameters which affect I_0 of the semiconductor, although the product $\sigma_n L_p$ is most likely to produce changes of orders of magnitude. Thus, the curves in Fig. 8 can be looked upon as caused by changes in the donor concentration N_D. With this assumption they correspond to the curves shown by Rittner.[4] However, it should be pointed out that it is preferable to consider the changes as the result of those in the product $\sigma_n L_p$ since L_p is not independent of $\sigma_n(N_D)$.[21,22]

Figure 10 shows $P_{\max}$ *vs* E_G for various conditions of atmospheric absorption. These curves are obtained by multiplying $\eta_{\max}$ from curves like those in Figs. 4 through 9 by the appropriate value of U, the total

[21] W. Shockley and W. T. Read, Phys. Rev. 87, 835 (1952).
[22] R. N. Hall, Phys. Rev. 87, 387 (1952).

power per cm² received from the sun under the same absorption conditions, i.e., $P_{\max}=\eta_{\max} U$.

LOAD IMPEDANCE FOR MAXIMUM POWER TRANSFER, R_{mp}

The load impedance at maximum power transfer can be shown to be

$$R_{mp}=\epsilon^{-\lambda V_{mp}}/\lambda I_0, \tag{15}$$

where I_0 and V_{mp} are computed as indicated in the preceding sections. Obviously R_{mp} is a function of E_G through I_0 and V_{mp}. In Fig. 11, we show R_{mp} *vs* E_G with I_s appropriate to a cloudy day, which will yield a representative picture of the variation of R_{mp} with E_G.

CONCLUSIONS

On the basis of the analysis presented here, the following conclusions concerning the choice of a material for solar energy converters can be made:

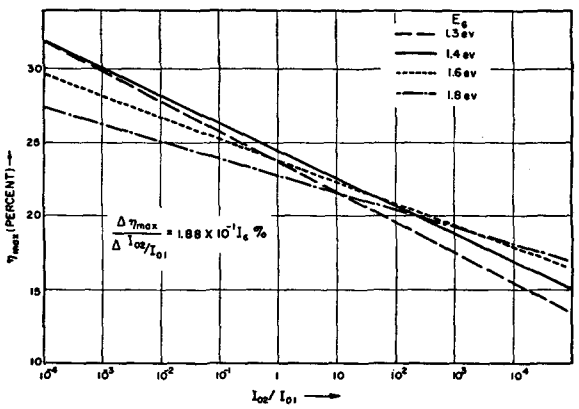

FIG. 8. $\eta_{\max}$ *vs* I_{02}/I_{01} for different values of E_G.

(1) If we confine ourselves to materials whose E_G is such that their maximum efficiency is greater than that of silicon, then it is never necessary to consider materials for which $E_G>2.2$ ev. (We shall designate this value of E_G as $E_{G\max}$.)

(2) $E_{G\max}$ becomes smaller as absorption of solar radiation by the atmosphere increases, e.g., when $m=3$, $w=0$, $E_{G\max}=1.5$ ev.

(3) Such increased absorption can result from atmospheric gases, from atmospheric humidity and from atmospheric dust. All these mechanisms for absorption tend to deplete the ultraviolet wavelengths, and therefore to shift the solar spectrum as the sun moves through the sky during the day and during the course of a year. Therefore, the best material for solar energy conversion changes with the time of day, time of year, and geographical location.

(4) $E_{G\max}$ never gets lower than about 1.5 ev, even under the most extreme conditions of absorption.

(5) The difference between silicon and the optimum material is greatest for conversion of solar energy outside the atmosphere. Under these conditions, $\eta_{\max}$ for Si is 19.2% while $\eta_{\max}$ for a material of $E_G=1.6$ ev is 24.6%. It is evident therefore that using the optimum material will not produce changes of order of magnitude in $\eta_{\max}$. It should be borne in mind, however, that Si has not achieved the $\eta_{\max}$ predicted for it theoretically. It is possible that some of the other materials may come closer to their theoretical values.

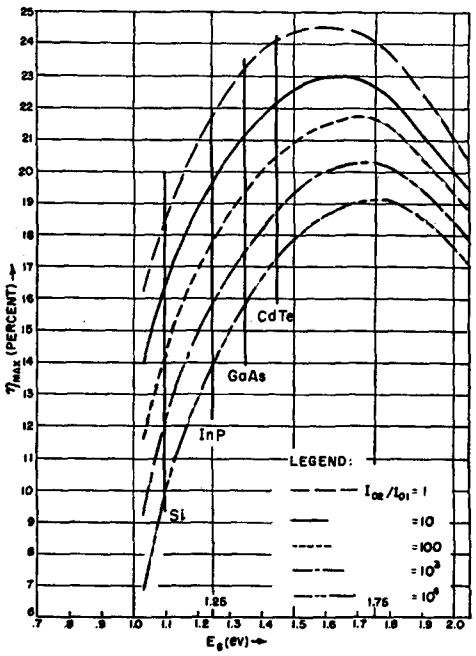

FIG. 9. $\eta_{\max}$ *vs* E_G, outside atmosphere ($m=0$, $w=0$) for different values of ratio I_{02}/I_{01}.

(6) The difference between $\eta_{\max}$ for Si and for the

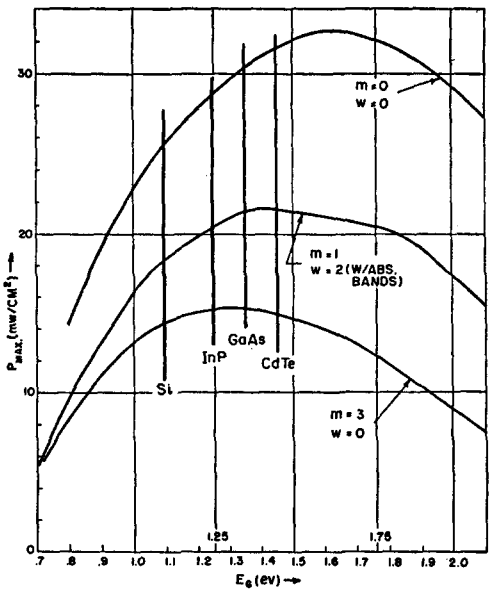

FIG. 10. Maximum power ($P_{\max}$) *vs* E_G for different absorption conditions.

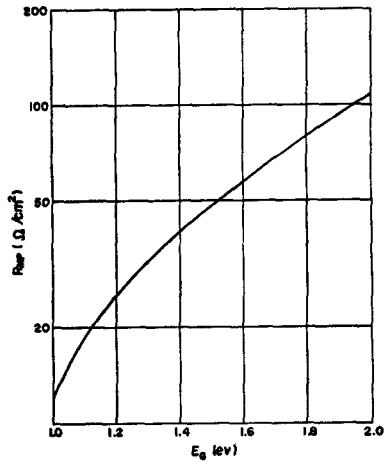

FIG. 11. Load resistance for maximum power transfer (R_{mp}) *vs* energy gap (E_G) with I_s computed for a cloudy day.

optimum material becomes less with increased absorption, i.e., when the sun is 70° from the zenith it is the difference between 19.3% and 20.5%.

(7) The difference would be further reduced if $I_0 \propto \exp -E_G/2kT$ instead of $I_0 \propto \exp -E_G/kT$ as we assumed throughout the analysis. There is reason to believe that in Si, $I_0 \propto \exp -E_G/2kT$, so that if any of the other materials realize the Shockley predicted dependence, they will enhance their advantage over Si.

(8) It does not appear as though any material for which 1.1 ev$<E_G<$1.5 ev will possess any advantage over silicon because of lower reflection losses, nor is there any reason to expect that any of these materials will ultimately have higher collection efficiency than the others. The combination of reflection losses and losses because of imperfect collection efficiency will reduce the practically attainable $\eta_{\max}$ by a factor between 0.7 and 0.5.

(9) Materials with larger values of E_G than Si place a less stringent requirement on r_s, the internal series resistance, since for such materials R_{mp} is greater than in Si.

(10) On the basis of the foregoing conclusions, it appears that semiconductors for which 1.1 ev$<E_G<$1.6 ev will be most likely to give higher $\eta_{\max}$ than Si. This conclusion is verified in Table III where it is shown that InP, GaAs, and CdTe, which have values of E_G in this range, have higher theoretical efficiencies than Si even in the present state of their technology. Even under the most unfavorable conditions of atmospheric absorption materials in this range of E_G values are at least as good as Si, and as atmospheric absorption decreases their advantage over Si increases.

(11) CdS photovoltaic cells should not be better than, or even as good as silicon. $\eta_{\max}$ of about 6% for CdS could be explained within the framework of this theory. It is possible, however, that the photovoltaic effect in CdS requires a different theoretical explanation as some of the reported experiments seem to indicate.[23]

(12) The difference between the results of Rittner and Prince can be readily explained by the solar spectral distribution they used.

ACKNOWLEDGMENTS

The author wishes to acknowledge many stimulating discussions with Mr. Paul Rappaport. He wishes to express appreciation to Dr. E. G. Linder for constant encouragement during the course of the work.

[23] These experiments were described in a paper delivered by D. C. Reynolds at the Conference on Solar Energy, Tucson, Arizona, November 1, 1955.